ELSEVIER

Biophysical Chemistry 123 (2006) 122–133

Biophysical Chemistry

http://www.elsevier.com/locate/biophyschem

Molecular mobility and dynamic site heterogeneity in amorphous lactose and lactitol from erythrosin B phosphorescence

Sonali Shirke, Yumin You, Richard D. Ludescher *

Department of Food Science, Rutgers, The State University of New Jersey, 65 Dudley Road, New Brunswick, NJ 08901-8520, United States

Received 22 March 2006; received in revised form 3 May 2006; accepted 4 May 2006
Available online 22 May 2006

Abstract

We have used phosphorescence from erythrosin B to characterize the molecular mobility and dynamic heterogeneity in dry films of amorphous lactose and lactitol from −25 to 120 °C. The phosphorescence emission spectra red-shifted and broadened with temperature in both sugars, indicating that both the rate of dipolar relaxation and the extent of inhomogeneous broadening increased dramatically at higher temperature. Phosphorescence intensity decays were well fit using a stretched exponential decay model; the rate constant for non-radiative quenching due to collisions with the matrix was calculated from the lifetimes. Arrhenius plots of this rate were non-linear, increasing very gradually at low and dramatically at high temperatures in both sugars. The rate of quenching was significantly lower in a 1:1 (wt/wt) mixture of lactose/lactitol in both the glass and the melt, providing strong evidence that specific interactions within the mixture lowered the matrix mobility. The lifetimes varied systematically with emission wavelength in both matrixes; analysis of the temperature dependence indicated that the activation energy for non-radiative quenching of the triplet state varied somewhat with emission wavelength. Time-resolved emission spectra collected as a function of delay time following pulsed excitation exhibited significant shifts to higher energy as a function of time. These data support a photophysical model in which erythrosin B molecules are distributed among matrix sites that vary such that blue-emitting sites with slower rates of matrix dipolar relaxation also have slower rates of molecular collisions. The amorphous matrixes of lactose and lactitol in both the glass and the melt state are thus characterized by dynamic site heterogeneity in which different sites vary in terms of their overall molecular mobility.

Keywords: Lactose and lactitol; Amorphous solid; Phosphorescence; Molecular mobility; Glass; Dynamic heterogeneity; Spectral heterogeneity

1. Introduction

Molecular mobility is generally thought to play an important, even crucial, role in modulating the stability and shelf-life of pharmaceuticals and solid foods and the viability of seeds and bacterial spores through its influence on the rate of molecular diffusion in amorphous solids; diffusion rates in turn modulate the rates of chemical reactions and physical processes [1–3]. The role of mobility in modulating the stability of biomaterials is usually addressed in terms of the glass transition temperature (T_g): foods are considered stable in the glass below T_g due to an absence of large-scale molecular motions that underlie flow and unstable in the melt or rubber above T_g due to the activation of such molecular motions. Although the T_g is a useful index temperature for stability in amorphous foods [1,4] and in seeds and grains [5,6], it is clear that the rates of chemical reaction and physical change are not solely controlled by T_g [7,8].

Molecular mobility within amorphous solids is usually discussed in terms of the relaxation modes originally identified in dielectric relaxation studies of synthetic polymers [9]. The relaxation activated at T_g, designated α and reflecting large-scale motions that underlie macroscopic flow, corresponds to whole molecule translational motions for small molecules and large-scale segmental motions for polymers. Relaxations activated at lower temperatures, designated β, γ, etc. from high to low temperature and activated at corresponding transition temperatures of T_β, T_γ, etc., correspond to more localized motions within the small molecule or progressively smaller segmental motions within the polymer. The literature

* Corresponding author. Tel.: +1 732 932 9611x231; fax: +1 732 932 6776.
E-mail address: ludescher@aesop.rutgers.edu (R.D. Ludescher).

0301-4622/$ - see front matter © 2006 Elsevier B.V. All rights reserved.
doi:10.1016/j.bpc.2006.05.001

characterizing the glass transition and its corresponding α relaxation, as well as β and other localized relaxations, in amorphous carbohydrates is extensive [4,10–18].

Amorphous solids, albeit non-crystalline and thus devoid of long-range molecular order, exhibit a range of structural features due to local differences in packing density or variations in the degree and strength of non-covalent interactions. Several, primarily spectroscopic, techniques [19–22] indicate that pure supercooled liquids and solids composed of either small molecules or polymers exhibit dynamic heterogeneity both through space and through time: the molecular dynamics throughout the matrix can differ significantly at any given time, while the molecular dynamics can fluctuate significantly through time at any given site. Data characterizing this spatial and temporal heterogeneity have included measurements of variations in the rates of mobility within the matrix or measurements of the size or fluctuation times characteristic of dynamically distinct sites [23–25]. The implications of this spatial and temporal heterogeneity for the macroscopic behavior of polymers or biomaterials have only been discussed recently [26–28].

Amorphous sugars and polyols also appear to exhibit dynamic heterogeneity. Slower than average β relaxation rates have been detected within a sub-ensemble of molecules selected by means of a spectroscopic filter in dielectric hole-burning experiments on amorphous D-sorbitol [29]. Diffusion measurements in highly viscous aqueous solution indicate that the translational self-diffusion coefficient follows a weaker than expected temperature dependence at temperatures near and above T_g in both sucrose [30] and maltose [31]; this behavior has recently been interpreted in terms of a physical picture of heterogeneous dynamics [20,22]. The size of the distinct dynamic regions in sorbitol have been estimated at 2.5 nm using NMR [32] and 3.6 nm using DSC [24].

We have recently demonstrated that phosphorescence from the dispersed probe erythrosin B (Ery B) provides a sensitive indicator of molecular mobility in amorphous sucrose [33], maltose and maltitol [34], and gelatin [35–37]. We have also shown that systematic variations in the phosphorescence lifetime across the emission band as well as blue shifts in the emission spectra with time following excitation provide a novel method of monitoring dynamic site heterogeneities in amorphous sucrose [33] and gelatin [36]. We report here a comparable phosphorescence study of molecular mobility and dynamic site heterogeneity in amorphous thin films of lactose and lactitol using steady-state emission and time-resolved intensity from dispersed Ery B. The data provide information on the rate of dipolar relaxation and collisional quenching within both the glass and the melt in these sugars. Surprisingly, we find that the molecular mobility of a 1:1 (wt/wt) mixture of lactose and lactitol had lower collisional quenching rates in both the glass and the melt than in either of its pure components, indicating that specific interactions among these similar molecules result in dynamic synergies that lower the molecular mobility of the components in the mixture. We also find that Ery B displayed spectral heterogeneity in thin films of amorphous lactose and lactitol, suggesting that dynamic site heterogeneities may be a general property of amorphous sugars.

2. Materials and methods

2.1. Sample preparation

Lactose and lactitol were purchased from Sigma-Aldrich (St. Louis, MO) with minimum purity of 98%. The free acid of erythrosin B (Ery B, tetra-iodo fluorescein) was dissolved in spectrophotometer grade dimethylformamide (DMF) to make a 10 mM solution; an aliquot from this solution was added to saturated aqueous sugar or sugar alcohol solutions to obtain dye/sugar molar ratios of $0.8{:}10^4$. A 1:1 mixture of lactose/lactitol was prepared from samples of lactose and lactitol containing dye.

To get glassy sugar films containing Ery B, 15 μl of dye–sugar solution were spread on a clean quartz slide 3 cm × 1.35 cm (NSG Precision Cells, Hicksville, NY), which was then dried for 5 min under a 1600 W hairdryer (Vidal Sassoon, NY). This method dried the films quickly without crystallization with a flow of ~90 °C air and heated the slide to a maximum temperature of ~88 °C (as measured by thermocouple probe). The thickness of the films was in the range of 10–40 μm as measured by micrometer (Mitutoyo Corp., Japan). The slides were stored in a desiccator containing P_2O_5 and DrieRite for at least 4 days prior to any luminescence measurements. All slides were checked for crystallization under crossed polarizers using a Nikon Type 102 dissecting microscope (Nikon, Inc., Japan). Since lactose readily crystallizes, wide-angle X-ray scattering patterns of lactose samples were obtained using a Bruker HiStar area detector and a rotating-anode X-ray generator equipped with a 0.5 mm collimator and a graphite monochromator (Cu Kα; $\lambda = 1.5418$ Å) operating at 40 kV and 75 mA. Multiple scans from amorphous lactose samples gave no indication of any crystalline material. Water content in films was determined by weighing samples before and after drying for 24 h at 70 °C in an Ephortee (Haake Buchler, Inc.) vacuum oven at 1000 mbar; lactose samples contained 1.48 ± 0.33 wt.% water, while lactitol samples contained 3.76 ± 0.4 wt.% water.

The glass transition temperature (T_g) of lactose is 104 °C [38–43] and of lactitol is 62 °C [44,45], based on averages of reported values. The glass transition temperature of a blend of lactose and lactitol can be estimated using the expression of Couchman and Karasz [46].

$$T_g = (x_1 T_{g1} + \kappa x_2 T_{g2})/(x_1 + \kappa x_2) \quad (1)$$

where x_1 and x_2 are the weight fraction of the components, κ is the ratio of heat capacity changes ($\Delta C_{p1}/\Delta C_{p2}$) at the glass transition, and T_{g1} and T_{g2} are the T_g's of the individual components. The ΔC_p value of lactose is 0.49 J K^{-1} g^{-1} [42], but there is no published value for lactitol; a $\Delta C_{p1}/\Delta C_{p2}$ ratio of 1.09, equal to that for maltose and maltitol [34], was thus used to estimate the T_g for a 1:1 mixture; the value, 82 °C, was relatively insensitive to this ratio.

2.2. Luminescence measurements and data analysis

All luminescence measurements were made using a Cary Eclipse Fluorescence Spectrophotometer (Varian Instruments, Walnut Creek, CA). A slide was fitted diagonally in a standard fluorescence cuvette, which was flushed with oxygen-free N_2 gas for at least 15 min prior to making measurements (O_2 will quench the triplet state). The temperature was controlled using a TLC 50 thermoelectric heating/cooling system (Quantum Northwest, Spokane, WA). For measurements below room temperature, a chamber surrounding the cuvette holder was flushed with dry air to eliminate moisture condensation.

Delayed fluorescence and phosphorescence emission spectra used excitation at 500 nm (bandwidth 20 nm) and emission was collected from 520 nm to 750 nm (bandwidth 10 nm). The emission intensity was collected from a single lamp flash over a 3 ms gate following a delay time of 0.1 ms. Delayed fluorescence and phosphorescence spectra were analyzed to obtain the peak frequency (ν_m) and the spectral bandwidth Γ (full width at half maximum) using a log-normal bandwidth function ($I(\nu)$) [47].

$$I(\nu) = I_o \exp\{-\ln(2)[\ln(1 + 2b(\nu-\nu_m)/\Delta)/b]^2\} \quad (2)$$

where I_o, ν_m, b and Δ are the peak intensity, peak frequency, asymmetry parameter and width parameter, respectively, for the emission band, and Γ was related to the width and asymmetry parameters as follows:

$$\Gamma = \Delta \sinh(b)/b \quad (3)$$

Luminescence spectra composed of both delayed fluorescence and phosphorescence bands were fit using a sum of two log-normal functions with independent fitting parameters.

The dipolar relaxation time (φ) was calculated from the temperature dependence of the phosphorescence emission peak $\nu_P(T)$ by analyzing the relaxation function

$$\frac{\Delta\nu}{\Delta\nu_r} = \frac{\nu(T)-\nu_{max}}{\nu_{min}-\nu_{max}} \quad (4)$$

where $\nu(T)$ is the emission peak energy at temperature T, ν_{min} is the peak energy at the lowest measured temperature and ν_{max} is the peak energy at the highest measured temperature. In a steady-state emission experiment, this relaxation function is the time average over the time-dependent relaxation of the matrix around the excited state, weighted by the phosphorescence intensity decay. Work by Richert [48] has indicated that the matrix dipolar relaxation around the triplet state is described by a stretched exponential function with time constant φ and stretching factor β_e; our results indicate that the intensity decay also follows a stretched exponential with time constant τ and stretching factor β_l (see below). The time average is thus given by the following integral:

$$\left\langle \frac{\Delta\nu}{\Delta\nu_r} \right\rangle = \frac{\int_0^\infty e^{-\left(\frac{t}{\varphi}\right)^{\beta_e}} e^{-\left(\frac{t}{\tau}\right)^{\beta_l}} dt}{\int_0^\infty e^{-\left(\frac{t}{\tau}\right)^{\beta_l}} dt} \quad (5)$$

whose solution for arbitrary β_e, β_l, α and φ is [34]:

$$\left\langle \frac{\Delta\nu}{\Delta\nu_r} \right\rangle = \frac{1}{\Gamma\left(\frac{1}{\alpha\beta}\right)} \frac{\alpha\varphi}{\tau + \alpha\varphi} = \frac{1}{\Gamma\left(\frac{1}{\beta_l}\right)} \frac{1}{1 + \frac{\beta_e}{\beta_l}\frac{\tau}{\varphi}} \quad (6)$$

Eq. (6) was solved for $\varphi(T)$ using measured values of $\tau(T)$ and $\beta_l(T)$ for Ery B (Fig. 6) and assuming that $\beta_e = 0.5$ based on work of Richert [48]; the relaxation rate plotted in Fig. 3 is the inverse of φ.

Phosphorescence emission spectra as a function of delay time following excitation at 500 nm (bandwidth 20 nm) were collected from 620 to 750 nm (bandwidth 10 nm). The emission intensity was collected from a single lamp flash over a 0.5 ms gate window following a delay time that varied from 0.1 ms to 2.5 ms; 10 cycles of excitation were averaged. Phosphorescence spectra were converted to intensity versus frequency (cm^{-1}) and analyzed to obtain the peak frequency (ν_m) and spectral bandwidth (Γ) using Eqs. (2) and (3).

To obtain intensity decays of Ery B in lactose and lactitol, the samples were excited at 530 nm (bandwidth 20 nm) and emission collected at 680 nm (bandwidth 20 nm) over the temperature range from −25 °C to 120 °C. Samples were equilibrated for 5 min at each temperature before collecting data. The intensity was collected as a function of time following the lamp flash over a window of 4 ms following a delay time of 0.1 ms and using a gate time of 0.02 ms; 10 cycles were summed to generate each decay transient. The intensity transients were analyzed using a stretch-exponential decay function:

$$I(t) = I(0)\exp[-(t/\tau)^{\beta}] + \text{constant} \quad (7)$$

where $I(0)$ is the initial intensity at time zero, t is the Kohlrausch–Williams–Watts lifetime [49] and β is the stretching exponent [50]. A detailed discussion of the appropriateness of this decay model is presented elsewhere [33]. Data analysis used the program NFIT (Island Products, Galveston, TX), which uses a non-linear least squares algorithm that varies the adjustable parameters to minimize χ^2. All fits gave R^2 values in the range of 0.99 to 1.0 and modified residuals ((data-fit)/data$^{1/2}$) plots that varied randomly about zero.

To obtain intensity decays of Ery B in lactose and lactitol as a function of emission wavelength, the samples were excited at 530 nm (bandwidth 20 nm) and emission collected as a function of emission wavelength from 640 to 720 nm (bandwidth 20 nm). The intensity was collected as a function of time following the lamp flash over a total window of 4 ms following a delay time of 0.1 ms and using a gate time of 0.02 ms; 10 cycles were summed to get a single decay. The intensity transients ($I(t)$) were analyzed using the stretch-exponential decay function (Eq. (7)).

2.3. Photophysical analysis

Our analysis of the photophysics of Ery B follows that of Duchowicz et al. [51], using slightly different nomenclature. The measured emission rate for phosphorescence ($k_P = 1/\tau$) is

the sum of all possible de-excitation rates for the triplet state T_1:

$$k_P = k_{RP} + k_{TS0} + k_{TS1} \quad (8)$$

where k_{RP} is the rate of emission to the ground state S_0, k_{TS0} is the rate of intersystem crossing to S_0 (rate of non-radiative quenching due to collisions with the matrix) and k_{TS1} is the rate of reverse intersystem crossing to the excited singlet S_1. (Oxygen quenching is assumed negligible due to the elimination of oxygen.)

The rate of radiative emission (k_{RP}) is 41 s^{-1} and constant [51,52]. The rate of reverse intersystem crossing to $S_1(k_{TS1})$ is a thermally activated process:

$$k_{TS1} = k^o_{TS1}\exp(-\Delta E_{TS}/RT) \quad (9)$$

where k^o_{TS1} is the maximum rate of intersystem crossing from T_1 to S_1 at high temperature, ΔE_{TS} is the energy gap between S_1 and T_1, R=8.314 J K^{-1} mol^{-1}, and T is the temperature in Kelvin. The magnitude of ΔE_{TS} was calculated from the slope of a Van't Hoff plot of the natural logarithm of the ratio of intensity of delayed fluorescence (I_{DF}) to phosphorescence (I_P) ($d[\ln(I_{DF}/I_P)]/d(1/T) = -\Delta E_{TS}/R$ where I_{DF} and I_P are the intensity values determined from analysis of the emission band using Eq. (2)). The value of $k^o_{TS1} = 6.5\times10^7$ s^{-1} for Ery B in aqueous solution [51]; however, this value has been found to be too large for Ery B in amorphous sucrose and other sugars [33]. We estimated that $k^o_{TS1} = 3.0\times10^7$ s^{-1} for Ery B in lactose and 6.5×10^7 s^{-1} in lactitol; these values essentially provide an upper estimate of the magnitude of k_{TS1} (T) and thus a lower limit on the calculated value of k_{TS0}.

The measured phosphorescence intensity (I_P) is proportional to the product of the quantum yield for formation of the triplet state (Q_T) and the probability of emission from the triplet state (q_P). Assuming that Q_T is constant (in absence of oxygen):

$$I_P \propto q_P = k_{RP}/(k_{RP} + k_{TS1} + k_{TS0}) \quad (10)$$

and

$$1/I_P \propto (k_{RP} + k_{TS1} + k_{TS0})/k_{RP} \quad (11)$$

Since k_{RP} is constant, this expression indicates that the decrease in intensity with temperature reflects an increase in the sum $k_{TS1}+k_{TS0}$; extensive curvature in a plot of $\ln(1/I_P)$ versus $1/T$ must, however, reflect a change in k_{TS0} since k_{TS1} follows Arrhenius behavior (Eq. (9)).

In analysis of the emission lifetimes as a function of emission wavelength, the magnitude of k_{TS1} made a minor contribution ($\leq\sim$15%) to the overall magnitude of k_P; Arrhenius analysis of $k_P(T)$ thus provided a reasonable estimate of the activation energy for collisional quenching (k_{TS0}).

3. Results

Previous spectroscopic studies have demonstrated that Ery B is dispersed throughout the sugar matrix and does not aggregate at the concentrations used in this study [33,53]. At a dye/sugar mole ratio of $\sim$0.8:10^4, each probe is on average surrounded by a matrix shell $\sim$10–11 sugar molecules thick. We are thus confident that the Ery B probe reports on the physical state of the unperturbed sugar matrix.

3.1. Phosphorescence emission

The delayed emission spectra from Ery B in amorphous lactose and lactitol (Fig. 1) include a phosphorescence band at long wavelengths (corresponding to the $S_0 \leftarrow T_1$ transition) and a thermally activated delayed fluorescence band at short wavelengths (corresponding to the $S_0 \leftarrow S_1 \leftarrow T_1$ transition). The ratio of delayed fluorescence to phosphorescence intensity increases systematically with temperature; a Van't Hoff analysis of the ratio of intensities was linear over the entire temperature range (with $R^2 > 0.995$ for all curves) and gave triplet–singlet activation energies (ΔE_{TS}) of 34.1±0.3 kJ mol^{-1} for lactose and 34.0±0.3 kJ mol^{-1} for lactitol. These energy gaps differ significantly from those seen for Ery B in amorphous sucrose (31.6±0.4 kJ mol^{-1}) [33] and maltose (32.7±1.1 kJ mol^{-1}) [34], in 66 wt.% aqueous sucrose (36.9±1.0 kJ mol^{-1}) [54], in ethanol (28.5±2.5 kJ mol^{-1}) [51], and in amorphous polyvinyl alcohol (41.2±0.4 kJ mol^{-1}) [52], but not in amorphous maltitol (34.2±0.9 kJ mol^{-1}) [34], suggesting that solvent (matrix) properties modulate the singlet–triplet energy gap.

The phosphorescence emission peak ν_P and bandwidth Γ_P, determined from analysis of the emission spectra using a log-normal function, varied systematically with temperature in both

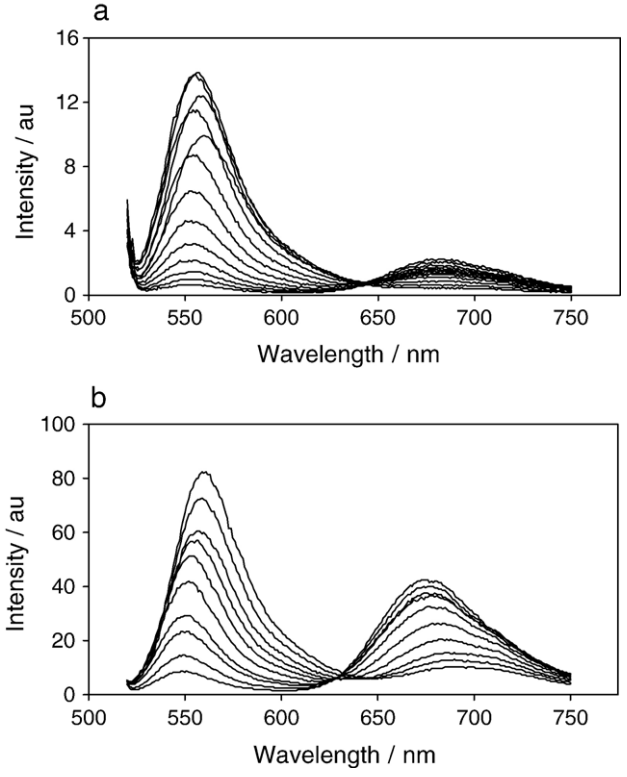

Fig. 1. Delayed emission spectra of Ery B dispersed in amorphous lactose (a) and lactitol (b). Spectra collected from 0 °C to 120 °C by 10 °C increments in lactose (high to low intensity at 680 nm) and from −5 °C to 15 °C and from 20 °C to 80 °C by 10 °C increments in lactitol (high to low intensity at 680 nm).

lactose and lactitol (Fig. 2). The Ery B emission energy was constant at low temperature in lactose, decreased gradually and linearly with temperature beginning at about 40 °C, and appeared to level off at ~90 °C (unfortunately, the signal intensity was too low to provide an estimate of the emission peak energy at higher temperatures). The thermal behavior in lactitol was different from that in lactose; the emission energy was significantly higher (~200 cm^{-1}) in the glass at low temperature, the energy decreased gradually at low temperature, and then more steeply at higher temperature. The dipolar relaxation rates for lactose and lactitol, calculated as described in Materials and methods, are plotted in an Arrhenius fashion in Fig. 3. These curves display upward curvature at higher temperatures, indicating that the activation energy increased with increasing temperature in both lactose and lactitol; these activation energies were 52 kJ mol^{-1} and 260 kJ mol^{-1} for lactose and 61 kJ mol^{-1} and 490 kJ mol^{-1} for lactitol at low and high temperature, respectively. The transition temperatures, corresponding to the break point temperatures in these curves and calculated from the intersection of the linear fits to low and high temperature data, were estimated as 36 °C for lactose and 44 °C for lactitol, both significantly below the T_g values of 104 °C and 62 °C for lactose and lactitol, respectively.

The thermal behavior of the bandwidth also differed in the two sugars. In lactose, the bandwidth increased very gradually at low temperature and then much more steeply at about 60 °C. In lactitol, on the other hand, the bandwidth was essentially constant at low temperature and only began to rise very gradually at about 60 °C.

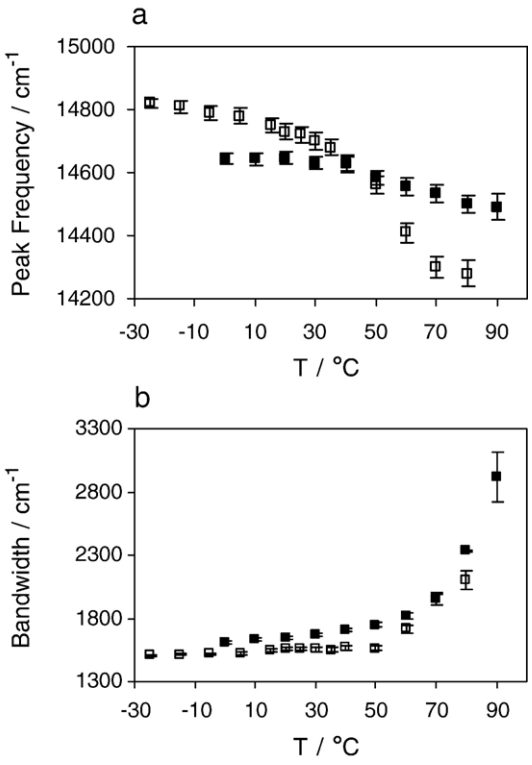

Fig. 2. Variation of phosphorescence emission peak frequency ν_P (a) and bandwidth Γ_P (b) with temperature in lactose (■) and lactitol (□). Parameters determined from fit of spectra (as in Fig. 1) to a log-normal function (Eq. (2), Materials and methods).

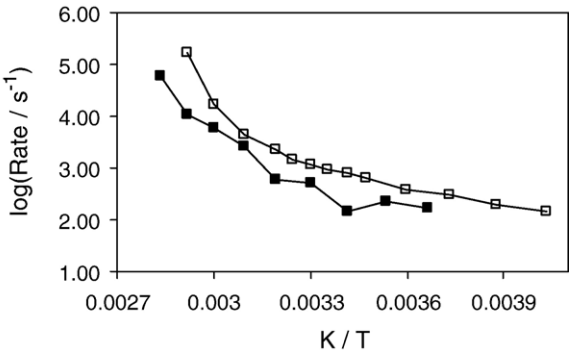

Fig. 3. Arrhenius plot of the effect of temperature on the rate of dipolar relaxation around the excited triplet state of erythrosin B in lactose (■) and lactitol (□). Relaxation rates calculated from analysis of the data in Fig. 2a as described in Materials and methods (Eq. (6)).

An Arrhenius-type analysis of the inverse phosphorescence intensity ($1/I_P$), where I_P was determined from a log-normal fit to the emission spectra, is plotted in Fig. 4. These curves are non-linear, indicating that novel quenching mechanisms were activated at higher temperatures. The transition temperatures (determined from intersection of lines fit to points at low and high temperature) were estimated as 83 °C for lactose and 33 °C for lactitol, both significantly below the respective T_g values for these sugars.

3.2. Phosphorescence intensity decays

The phosphorescence emission decays from Ery B in amorphous lactose and lactitol at −25 °C are plotted in Fig. 5. These decays were well fit using a stretched exponential decay model in which the Kohlrausch–Williams–Watts lifetime τ and the stretching exponent β are the physically meaningful parameters. A stretched exponential decay model has provided both a statistically and a theoretically satisfying description of the intensity decay of Ery B in amorphous sugars [33,34] and proteins [35–37]. All intensity decays collected as a function of

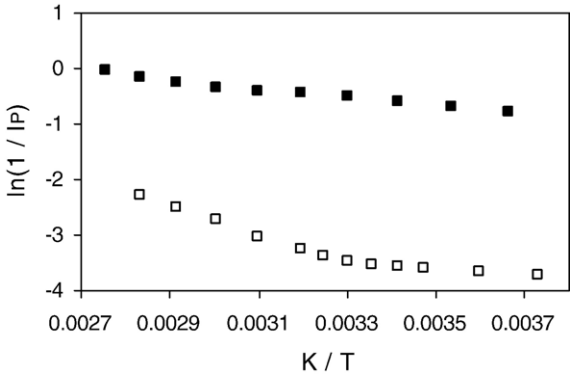

Fig. 4. Arrhenius-type plot of the effect of temperature on the phosphorescence emission intensity I_P of Ery B in lactose (■) and lactitol (□). The value of I_P was determined from a fit of spectra (as in Fig. 1) to a log-normal function (Eq. (2), Materials and methods).

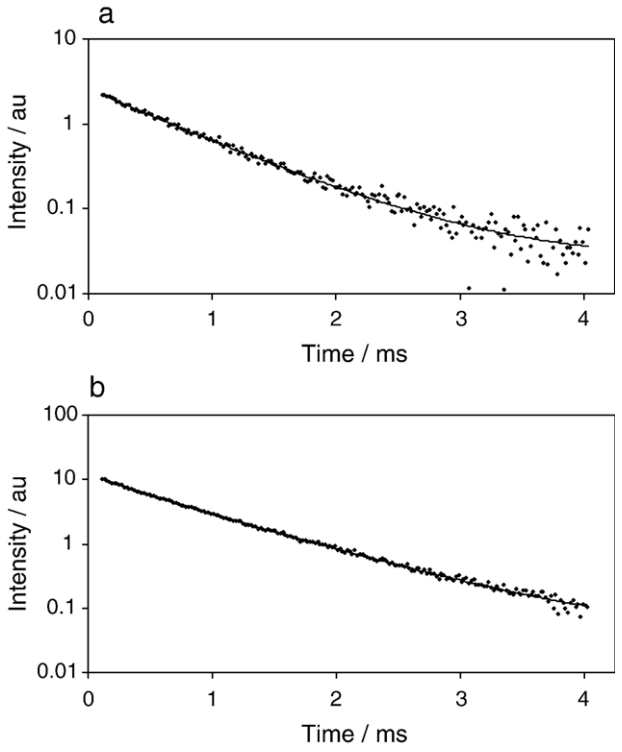

Fig. 5. Phosphorescence emission intensity decay transients ($I_P(t)$) from Ery B in amorphous lactose (a) and lactitol (b) at −25 °C; solid lines are calculated fits using a stretched exponential function (Eq. (7), Materials and methods) with τ=0.675 ms and β=0.957 for lactose and τ=0.671 ms and β=0.920 for lactitol.

temperature in the temperature range from −25 °C to 120 °C in lactose and lactitol were well fit using a stretched exponential decay model; the fit lifetimes and stretching factors are plotted versus temperature in Fig. 6. The lifetimes decreased as a function of temperature from ~0.67 ms at −25 °C in both sugars to 0.28 ms in lactitol at 80 °C and 0.16 ms in lactose at 120 °C. The lifetimes in lactose and lactitol were similar over the temperature range from −25 °C to ~30 °C; however, at 35 °C and above, the lifetimes in lactitol were significantly lower than those in lactose. The stretching exponent β was approximately constant at 0.9–0.95 over the entire temperature range in both sugars.

Interpretation of Ery B lifetimes as a function of temperature is complicated by thermally activated reverse intersystem crossing that modulates the lifetime. The photophysical rate constants for de-excitation of the triplet state of Ery B in lactose and lactitol, calculated from the lifetimes and estimates of the reverse intersystem crossing rate k_{TS1}, are plotted versus temperature in Fig. 7. In both sugars, the total de-excitation rate k_P (=1/τ) increased gradually at low temperature and more steeply at higher temperature; the correction for the reverse intersystem crossing rate k_{TS1} was relatively minor for Ery B in lactitol (~5% at the highest temperature) but more significant in lactose (~18% at the highest temperature); the calculated values of the collisional quenching rate k_{TS0} increased gradually at low and more steeply at high temperature for both lactose and lactitol. The variation of k_{TS0} with temperature for lactose, lactitol and for a 1:1 mixture of lactose/lactitol, calculated from the Ery B lifetime in a manner identical to that illustrated in Fig. 7, are plotted as log(k_{TS0}) versus 1/T in Fig. 8. The activation energies for k_{TS0} in lactose, lactitol and the mixture, respectively, were 1.67, 1.86 and 1.01 kJ mol^{-1} at low, and 43.5, 14.2 and 45.3 kJ mol^{-1} at high temperature while the transition temperatures, calculated from the intersection of the trend lines at low and high temperature, were 94 °C in lactose, 21 °C in lactitol and 93 °C in the mixture. Interestingly, the quenching rate in the mixture was not intermediate between that for lactose and lactitol, but rather was lower than in either pure sugar over nearly the entire temperature range from −10 to 90 °C.

3.3. Wavelength dependence of phosphorescence lifetimes

All erythrosin B intensity decays collected as a function of emission wavelength from 640 to 720 nm and temperature from −25 to 100 °C in both lactose and lactitol were well fit using the stretched exponential model. The variation of τ with emission wavelength is plotted in Fig. 9 at selected temperatures for the sake of clarity. The lifetimes varied with emission wavelength in both lactose and lactitol. In lactose, the lifetimes at 20 °C ranged from a high of 0.76 ms at 640 nm to a low of 0.57 ms at 720 nm; lifetimes also decreased monotonically with increasing wavelength at 40 °C. In the temperature interval from 50 °C to 90 °C, however, lifetimes increased with increasing wavelength at the blue edge to a maximum at 660–670 nm and then decreased at

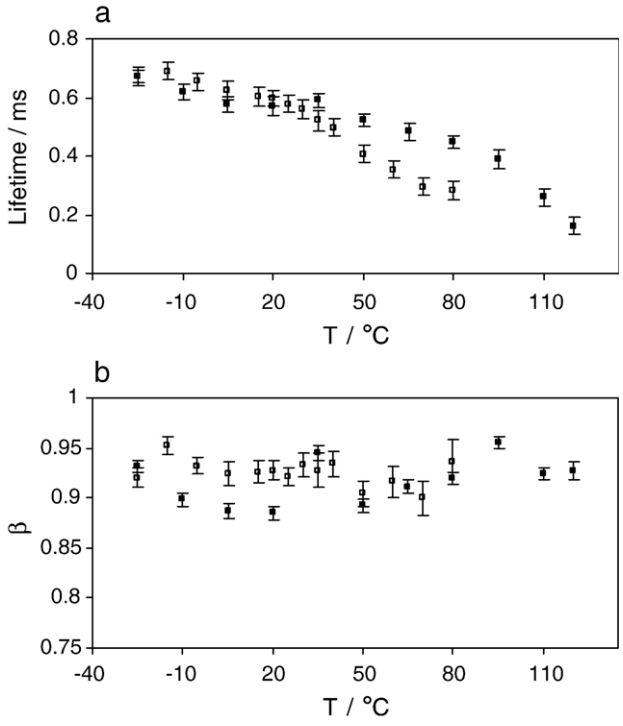

Fig. 6. Effect of temperature on the lifetime τ (a) and stretching exponent β (b) from stretched exponential analyses (see Materials and methods) of phosphorescence from Ery B in amorphous lactose (■) and lactitol (□).

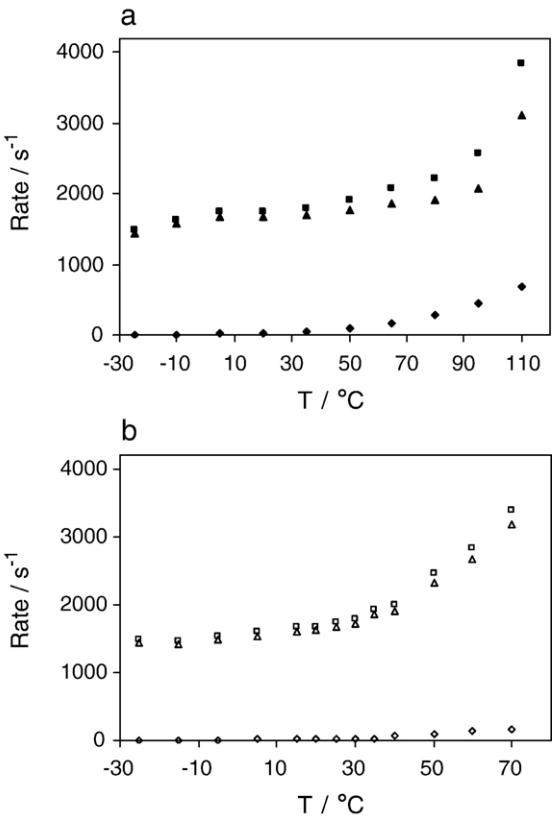

Fig. 7. Effect of temperature on the rate constants for de-excitation of the triplet state of Ery B in amorphous lactose (a) and lactitol (b); the rates plotted are k_P (■, □), k_{TS1} (♦, ◇) and k_{TS0} (▲, △) (see text for details).

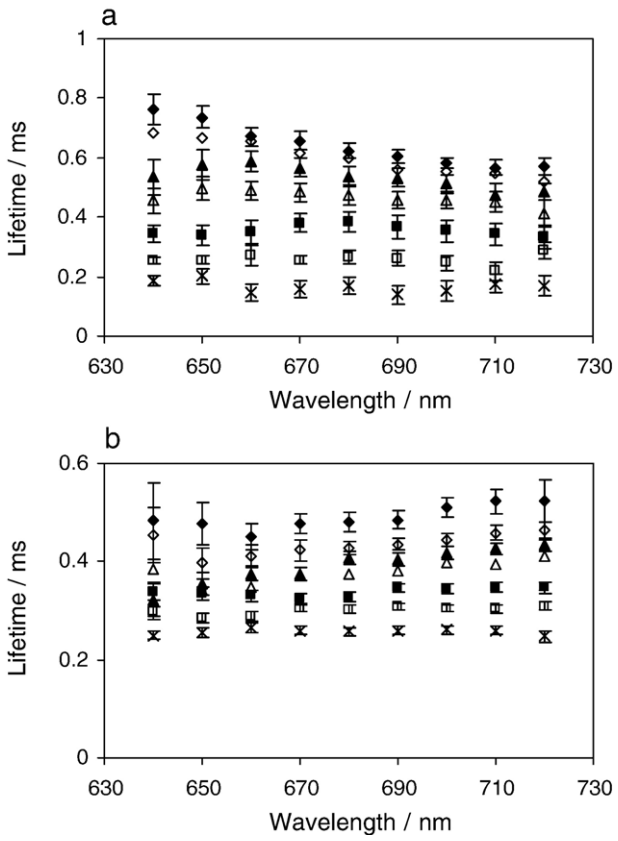

Fig. 9. Effect of emission wavelength on Ery B phosphorescence lifetimes in amorphous lactose (a) and lactitol (b); lifetimes determined from analysis of intensity decay transients using a stretched exponential model (see text for details). Data collected at 20 °C (♦), 40 °C (◇), 60 °C (▲), 80 °C (△), 100 °C (■), 110 °C (□) and 120 °C (×) for lactose, and at −25 °C (♦), −10 °C (◇), 20 °C (▲), 40 °C (△), 70 °C (■), 80 °C (□) and 90 °C (×) for lactitol.

higher wavelengths, while at 100 °C and above the lifetimes were approximately constant with emission wavelength. In lactitol, the lifetimes at −25 °C varied from high values of 0.48 ms and 0.52 ms at 640 and 720 nm to a low of 0.45 ms at 660 nm; a similar pattern persisted up to 40 °C but at higher temperatures the lifetimes were essentially constant with emission wavelength. Comparable or larger variations in the lifetime with emission wavelength have been reported previously for this probe in amorphous sucrose [33], in amorphous maltose and maltitol [34], and in gelatin [35] and for a similar xanthene probe, eosin, in amorphous sucrose at ambient temperatures [54] and in glycerol at cryogenic temperature [55].

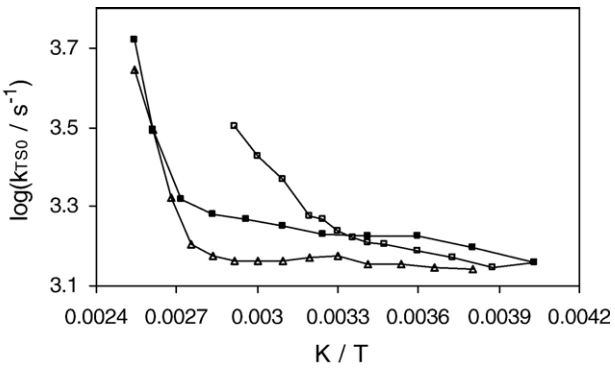

Fig. 8. Arrhenius plot of the non-radiative decay rate (k_{TS0}) for the triplet state of Ery B in amorphous lactose (■), lactitol (□) and the 1:1 mixture of lactose/lactitol (△) as a function of inverse temperature.

The variation in lifetime must reflect variations in the underlying photophysical rate constants as a function of emission wavelength. As discussed in a previous study of Ery B in amorphous sucrose [33], any variations in k_{RP} due its dependence on ν^3 or k_{TS1} due to variations in ΔE_{TS} would generate a systematic increase in lifetime with emission wavelength at all temperatures. It thus seems probable that the variations in lifetime with emission wavelength reflect variations in the non-radiative rate constant k_{TS0} with wavelength. Given that the lifetime decreases, and thus k_{TS0} increases, with increasing wavelength under some conditions, this variation cannot solely reflect a dipolar relaxation mechanism in which longer lived chromophores have red-shifted emission [56–58]. Arrhenius analysis of the temperature dependence of the rate constant k_P ($=1/\tau$) at each wavelength provides an estimate of the apparent activation energy (E_A) for non-radiative quenching (k_{TS0}). These values for lactose and lactitol in the glass at low and in the melt at high temperature are plotted in Fig. 10.

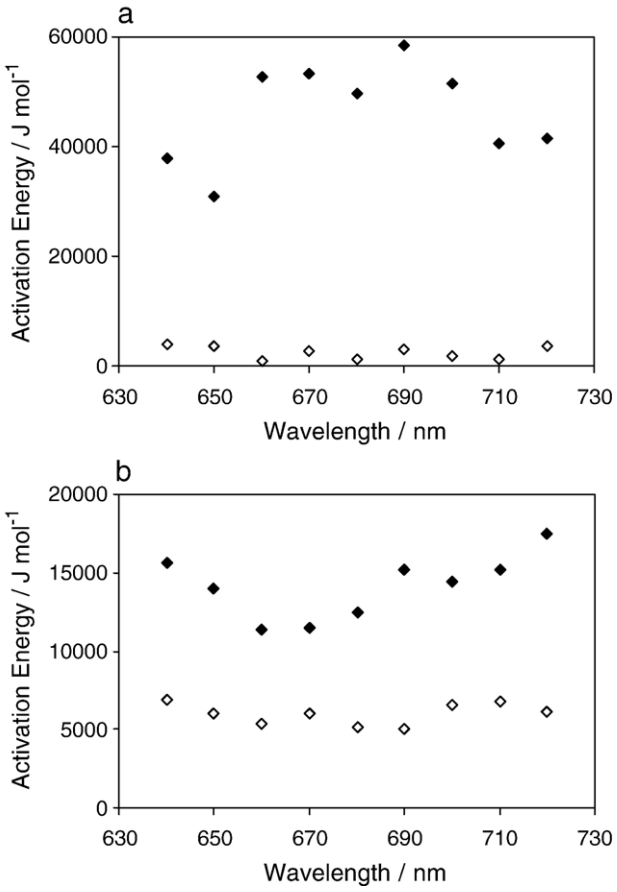

Fig. 10. Variation of activation energy (E_A) for quenching of phosphorescence lifetime of erythrosin B in amorphous lactose (a) and lactitol (b) at temperatures below (◇) and above (♦) the glass transition temperatures.

The activation energy for non-radiative quenching was about 10-fold higher in the melt at high temperature than in the glass at low temperature in lactose and about three-fold higher in lactitol. Values in lactose varied from 0.7 to 4.0 kJ mol^{-1} at low temperature and from 31 to 58 kJ mol^{-1} at high temperature. Although E_A was higher at short wavelength in the glass, E_A was higher at intermediate wavelength in the melt. In lactitol, E_A ranged between 5.1 and 6.8 kJ mol^{-1} in the glass with no apparent systematic variation with wavelength, but varied systematically from high values of 15.7 and 17.5 kJ mol^{-1} at 640 and 720 nm, respectively, to a low of 11.4 kJ mol^{-1} at 660 nm in the melt. Similar variations in E_A with emission wavelength for Ery B have been seen in other amorphous biomaterials including sucrose [33], maltose and maltitol [34], and gelatin [36].

The stretching exponent β also varied with emission wavelength at several temperatures for both lactose and lactitol (data not shown). In lactose, β varied randomly in the range from 0.8 to 0.95 across the emission band with generally smaller values at higher temperatures. In lactitol, however, β varied over a similar range at the blue edge of the emission band from 640 to 670 nm but was essentially constant at higher wavelengths; temperature had a significant affect on β only at the blue edge of the emission band.

3.4. Time-resolved phosphorescence emission spectra

The variations in phosphorescence lifetime with emission wavelength provide indications that the emission spectrum and lifetime of dye molecules are coupled within these sugar matrixes. We have shown in a previous study of amorphous sucrose using Ery B phosphorescence [33] that long lifetime chromophores have blue-shifted phosphorescence emission and short lifetime chromophores have red-shifted emission; a similar correlation was found to exist in maltose and maltitol [34], in gelatin [36], and may also exist in lactose and lactitol. This prediction was tested by collecting time-resolved emission spectra for Ery B as a function of delay time over the time window from 0.1 to 2.5 ms. The emission peak frequency (ν_P) for these spectra are plotted versus delay time in Fig. 11. The peak frequency shifted to higher energy (blue-shifted) with increasing delay time in both lactose and lactitol; these shifts were approximately linear in time and of consistent magnitude (~200 cm^{-1}) at all temperatures measured from −10 °C to 80 °C in lactose and from −10 °C to 45 °C in lactitol. All curves were approximately parallel in both sugars; vertical shifts with temperature reflected additional stabilization of the triplet state at higher temperature due to increasing dipolar relaxation rate [33,34,59]. At short time (0.1 ms delay), the spectra reflected emission from all chromophores (weighted

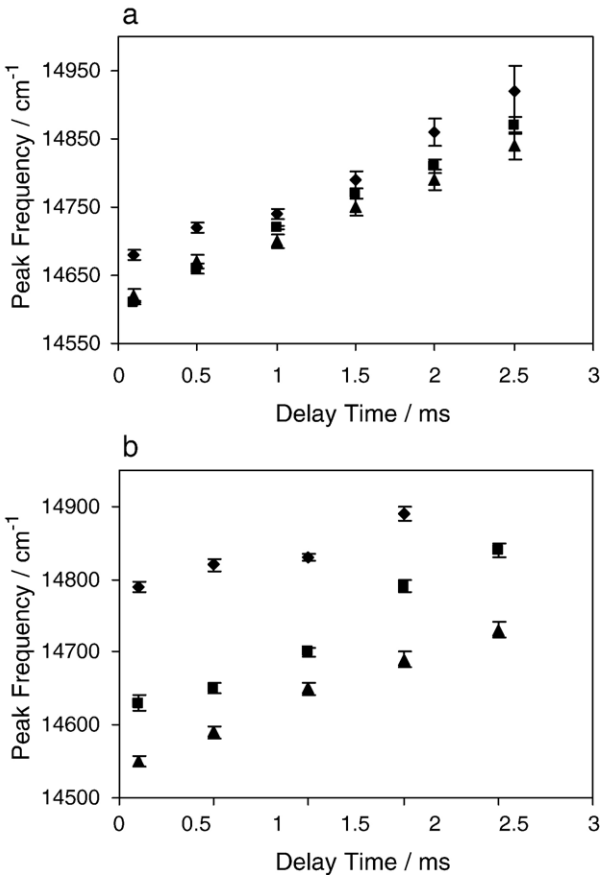

Fig. 11. Evolution of phosphorescence emission peak frequency ν_P with time following excitation in amorphous lactose (a) at −10 °C (♦), 40 °C (■) and 80 °C (▲), and in amorphous lactitol (b) at −10 °C (♦), 20 °C (■) and 45 °C (▲).

by their absorbance and inverse lifetime); at long time (2.5 ms delay), however, the measured spectrum only reflected emission from long-lived chromophores. These data thus provide direct evidence that the emission from Ery B in these amorphous sugar matrixes is spectrally correlated such that probes in environments with shorter lifetimes have red-shifted emission spectra and probes in environments with longer lifetimes have blue-shifted emission spectra.

Analysis of the emission bandwidth Γ_P indicated that there was a consistent increase with increasing delay time in lactose at low but not at high temperature and only a slight increase in Γ_P with delay time in lactitol at low temperature (data not shown). These data indicate that the extent of inhomogeneous broadening, due to a broadening of the distribution of matrix environments, was larger for chromophores with blue-shifted emission spectra in both lactose and lactitol at low temperature.

4. Discussion

The phosphorescence emission wavelength and intensity of Ery B in amorphous solid sucrose [33,60], maltose and maltitol [34], and gelatin [36,37] are influenced by two general modes of matrix molecular mobility that modulate the energy and lifetime of the excited triplet T_1 state: dipolar relaxation and collisional quenching. Our discussion of how the phosphorescence properties of Ery B provide information about molecular mobility in amorphous lactose and lactitol builds on this background.

The peak frequency of the phosphorescence emission decreased 150 cm^{-1} in lactose and 540 cm^{-1} in lactitol over a temperature range of ~100 °C. These decreases, which are comparable to those seen for Ery B in amorphous sucrose (~350 cm^{-1}) [33] and in maltose and maltitol (~300 cm^{-1} and ~500 cm^{-1}, respectively) [34], are consistent with a dipolar relaxation mechanism around the excited triplet state [58]. In amorphous solid sugars, dipolar relaxation reflects mobility of the sugar hydroxyl groups due either to localized (segmental) motions associated with the β relaxations activated at low temperature in the glass or to large-scale α relaxations associated with flow activated at T_g. Interestingly, the magnitude of the dipolar relaxation (that is, the total decrease in emission energy) appears to be significantly larger in lactitol (and maltitol) than in lactose (and maltose); this may be related to the larger intensity of the β relaxation seen in sugar alcohols than in their corresponding sugars [14,16]. The activation energies calculated from Arrhenius analysis of the dipolar relaxation rate for lactose and lactitol, 52 and 61 kJ mol^{-1} at low temperature, and 260 and 490 kJ mol^{-1} at high temperature, respectively, were comparable to those reported for the β and α relaxations of the similar disaccharide maltose, 45 and 405 kJ mol^{-1} [16]. (Unfortunately, there are no dielectric studies in the literature of amorphous dry lactose or lactitol.) Although the calculated dipolar relaxation rates at high temperature (~10^4 to 10^5 s^{-1}) are comparable to those expected for the α relaxation in disaccharides [16,61], the rates at low temperature (10^2 to 10^3 s^{-1}) are 3–4 orders of magnitude slower than β relaxations reported for other sugars [17]. However, since the width of the β relaxation is 3–4 orders of magnitude, it is possible that only very slow components of the β relaxation actually contribute to dipolar relaxation in these sugars. A similar discrepancy between dipolar and dielectric relaxation rates in the glass but not the melt was seen in maltose and maltitol [34].

Dipolar relaxation rates are usually monitored by direct observation of a red-shift in the emission spectrum as a function of time following pulsed excitation [56,58]. In these amorphous matrixes, as in all the amorphous matrixes we have analyzed using the Ery B probe, such measurements were not possible because the emission blue shifts with time following excitation. This phenomenon, which provides insight into the dynamic heterogeneity within the amorphous solid, is discussed below.

The emission intensity (I_P) and the lifetime (τ) are directly modulated by the rates of radiative emission k_{RP}, of reverse intersystem crossing to the excited singlet state k_{TS1} and of intersystem crossing to the ground singlet state k_{TS0}. The value of k_{RP} is 41 s^{-1} for Ery B [51,52], while k_{TS1} follows Arrhenius kinetics. The rate of intersystem crossing k_{TS0}, which is modulated by the physical state of the amorphous matrix [33,37,62], reflects both the manner in which the excited T_1 state of Ery B is vibrational coupled to the S_0 ground state as well as the manner in which the ground state vibrational energy can dissipate from the excited probe into the surrounding matrix [63]. Since the efficiency of this vibrational dissipation is related to the overall mobility of the matrix [64], k_{TS0} provides a direct measure of matrix mobility.

The magnitude of k_{TS0} in lactose was ~1450 s^{-1} at −25 °C and increased gradually up to about 90 °C and then dramatically at higher temperature; this behavior was similar to that seen in amorphous sucrose and maltose and certainly reflects the activation of α relaxations at T_g. The magnitude of k_{TS0} in lactitol was also ~1450 s^{-1} at −25 °C and increased gradually up to about 20 °C, and then more steeply at higher temperature; in this case, given the low temperature of the transition, significantly below the T_g, the increase may reflect more complex dynamic behavior in the lactitol glass. This conclusion is uncertain, however, since the lactitol T_g may be reduced significantly in the presence of residual water (3.8%).

The magnitude of k_{TS0} in the 1:1 mixture of lactose/lactitol was not intermediate between that of pure lactose and lactitol but rather was lower over the entire temperature range. Specific interactions between lactose and lactitol thus significantly decreased the molecular mobility of the mixed amorphous matrix. A similar dynamic synergy has been seen in amorphous mixtures of maltose and maltitol where the mobility of the 7:3 and 1:1 mixtures (maltose/maltitol) was lower than that seen in either pure component [34].

This lower mobility in the 1:1 mixture is comparable to the phenomenon of antiplasticization seen in amorphous synthetic polymers where low concentrations of small molecules make the polymer matrix more rigid, less elastic or less permeable [65,66]. Similar antiplasticization effects have been reported in amorphous biomaterials including starch films containing glycerol [67] and sorbitol [68,69] as well as plasticized freeze-dried powders of polyvinyl pyrolidone, dextran and

ficoll [70]. Some studies of stability in amorphous foods in the presence of small amounts of water or other plasticizers may also be explainable in terms of the antiplasticization phenomenon [71].

Antiplasticization may be the result of a negative volume change on mixing which decreases the free volume and the molecular mobility in both synthetic polymers [72] and in carbohydrates [73]. There are suggestions from studies of synthetic polymers [74] and carbohydrates, including starch [68] and maltose [75], that the effect may be a consequence of the suppression of β relaxations within the glass.

Previous reports of antiplasticization behavior have been largely confined to mixtures of molecules of dissimilar sizes (and glass transition temperatures). However, given that a similar decrease in molecular mobility has been detected in mixtures of maltose and maltitol using this phosphorescence method [34], such dynamic synergy as we report here may also be a common feature of mixtures of even quite similar biomolecules. If so, such dynamic synergies have real implications for understanding how the composition of an amorphous matrix modulates the local molecular mobility and thus the long-term stability of pharmaceuticals and solid foods [2,3] and perhaps the viability of seeds and bacterial spores [76].

The spectral heterogeneities reported here for Ery B phosphorescence provide information about the heterogeneity of the matrix environment in amorphous lactose and lactitol. These spectral features are similar to those reported previously for the same probe in amorphous sucrose, maltose and maltitol, and gelatin. We thus propose an essentially similar photophysical model to explain the spectral heterogeneities in lactose and lactitol, a model in which Ery B molecules are distributed among a continuum of preexisting matrix sites that differ in terms of their overall molecular mobility.

In the standard relaxation model for spectral heterogeneity, longer lifetime probes have red-shifted emission due to more extensive dipolar relaxation around the longer lived excited states [56–58]; a decrease in lifetime across the emission band is not consistent with this model. We thus propose a dynamic site heterogeneity model in which probes are distributed among dynamically distinct matrix sites [33]. In this model, probe molecules with blue-shifted emission, which have higher energy triplet states, are in matrix sites with slower dipolar relaxation rates. Probes with red-shifted emission, which have lower energy triplet states, are in sites with faster dipolar relaxation rates. A distinctive feature of this model is that probes in sites with blue-shifted emission have longer lifetimes and thus smaller values of k_{TS0}, while probes in sites with red-shifted emission have shorter lifetimes and thus larger values of k_{TS0}.

In amorphous sucrose, and to a lesser extent in amorphous maltose and maltitol, red-shifted sites have lower activation energies for molecular collisions that promote de-excitation of the excited state. In hydroxylated solvents, the magnitude of the activation energy has been related to the size of the reorienting unit that controls the relaxation rate [77]. Higher values of E_A thus provide evidence that the molecular collisions that activate non-radiative quenching in these sugar matrixes involve larger cooperative units; that is, that collisional quenching involves the collective motion of larger molecular groups. Although there are indications from the variation of E_A with wavelength that different matrix sites may have distinct activation energies in lactose at low temperature and in lactitol at high temperature, the evidence for such dynamic complexity in these sugars is weak.

The values of the stretching exponent β vary in the range from 0.8–0.95 in both lactose and lactitol. The Ery B probes thus appear to be distributed among a continuum of matrix sites that differ in the rate of collisional quenching k_{TS0} and thus differ in matrix mobility. A continuous distribution, rather than discrete classes of sites, is compatible with the known properties of amorphous solids [78,79].

The following photophysical model thus appears to describe how Ery B monitors the physical state of amorphous solid lactose and lactitol. Probes are distributed among a continuum of matrix environments ranging from more rigid (blue-shifted emission) to more mobile (red-shifted emission) sites. Rigid sites have slower dipolar relaxation rates and slower collisional quenching rates; these sites of lower overall molecular mobility may be physical regions of the amorphous matrix that are organized into larger aggregates of more strongly interacting sugar molecules, probably due to more extensive hydrogen bonding. Mobile sites, on the other hand, have faster dipolar relaxation rates and faster collisional quenching rates; these sites of higher overall molecular mobility may be physical regions of the amorphous matrix that are organized into smaller aggregates of weakly interacting sugar molecules, probably due to less extensive hydrogen bonding. Although this study provided little information about the temporal and spatial continuity of these regions, they must have persistence times longer than the excited triplet state lifetime of ≤ 1 ms and spatial extents larger than the ~ 1 nm linear dimension of an erythrosin molecule [80].

Spectral heterogeneities in Ery B phosphorescence thus support a physical model for dynamic site heterogeneities within amorphous lactose and lactitol that is remarkably consistent with the physical model generated for supercooled liquids and amorphous polymers both below and above the glass transition temperature [19–22]. Given similar spectral heterogeneity for erythrosin B in amorphous sucrose, maltose and maltitol, and gelatin and for eosin in glycerol at cryogenic temperature [55], the existence of such dynamic site heterogeneities may be a consistent feature of the amorphous state of solid sugars, sugar alcohols and perhaps other polyols; if so, this dynamic site heterogeneity must certainly be incorporated into any detailed physical chemical description of the stability of amorphous biomaterials [28].

Acknowledgements

This research was supported by grants (#2001-01683 and #2002-01585) from the National Research Initiative of the United States Department of Agriculture. Sonali Shirke gratefully acknowledges the support of the Mid-Atlantic Consortium and the E.W. Kellogg Foundation.

References

[1] O.R. Fennema, in: O.R. Fennema (Ed.), Food Chemistry, 3rd ed., Water and Ice, Marcel Dekker, Inc., NY, 1996, pp. 17–94.
[2] Y.H. Roos, Phase Transitions in Foods, Academic Press, San Diego, 1995.
[3] D. Champion, M. Le Meste, D. Simatos, Towards an improved understanding of glass transition and relaxations in foods: molecular mobility in the glass transition range, Trends Food Sci. Technol. 11 (2000) 41–55.
[4] H. Levine, L. Slade, Physical chemistry of foods, in: H.G. Schwartzberg, R.W. Hartel (Eds.), Glass Transitions in Foods, Marcel Dekker, Inc., NY, 1992, pp. 83–222.
[5] M.J. Burke, in: A.C. Leopold (Ed.), Membranes, Metabolism, and Dry Organisms, The Glassy State and Survival of Anhydrous Biological Systems, Cornell University Press, NY, 1986, pp. 358–364.
[6] W.Q. Sun, A.C. Leopold, Glassy state and seed storage ability: a viability equation analysis, Ann. Bot. 74 (1994) 601–604.
[7] G. Roudaut, M. Maglione, D. van Dusschoten, M. Le Meste, Molecular mobility in glassy bread: a multispectroscopy approach, Cereal Chem. 76 (1999) 70–77.
[8] G. Roudaut, M. Maglione, M. Le Meste, Relaxations below glass transition temperature in bread and its components, Cereal Chem. 76 (1999) 78–81.
[9] N.G. McCrum, B.E. Read, G. Williams, Anelastic and Dielectric Effects in Polymeric Solids, John Wiley & Sons, London, 1967.
[10] L. Slade, H. Levine, A food polymer science approach to structure–property relationships in aqueous food systems: non-equilibrium behavior of carbohydrate–water systems, Adv. Exp. Med. Biol. 302 (1991) 29–101.
[11] T.R. Noel, S.G. Ring, M.A. Whittam, Glass transitions in low-moisture foods, Trends Food Sci. Technol. 1 (1990) 62–67.
[12] R.K. Chan, K. Pathmanathan, G.P. Johari, Dielectric relaxation in the liquid and glassy states of glucose and its water mixtures, J. Phys. Chem. 90 (1986) 6358–6362.
[13] T.R. Noel, S.G. Ring, M.A. Whittam, Dielectric relaxations of small carbohydrate molecules in the liquid and glassy states, J. Phys. Chem. 96 (1992) 5662–5667.
[14] Gangasharan, S.S.N. Murthy, Study of α-, β-, and γ-relaxation processes in some supercooled liquids and supercooled crystals, J. Chem. Phys. 99 (1993) 9865–9873.
[15] T.R. Noel, R. Parker, S.G. Ring, A comparative study of the dielectric relaxation behavior of glucose, maltose, and their mixtures with water in the liquid and glassy states, Carbohydr. Res. 282 (1996) 193–206.
[16] T.R. Noel, R. Parker, S.G. Ring, Effect of molecular structure and water content on the dielectric relaxation behavior of amorphous low molecular weight carbohydrates above and below their glass transition, Carbohydr. Res. 329 (2000) 839–845.
[17] A. Faivre, G. Niquet, M. Maglione, J. Fornazero, J.F. Jal, L. David, Dynamics of sorbitol and maltitol over a wide time–temperature range, Eur. Phys. J. B 10 (1999) 277–286.
[18] L. Carpentier, M. Descamps, Dynamic decoupling and molecular complexity of glass-forming maltitol, J. Phys. Chem., B 107 (2003) 271–275.
[19] H. Sillescu, Heterogeneity at the glass transition: a review, J. Non-Cryst. Solids 243 (1999) 81–108.
[20] M.D. Ediger, Spatially heterogeneous dynamics in supercooled liquids, Annu. Rev. Phys. Chem. 51 (2000) 99–128.
[21] H. Sillescu, R. Böhmer, G. Diezemann, G. Hinze, Heterogeneity at the glass transition: what do we know? J. Non-Cryst. Solids 307–310 (2002) 16–23.
[22] R. Richert, Heterogeneous dynamics in liquids: fluctuations in space and time, J. Phys., Condens. Matter 14 (2002) R738–R803.
[23] K. Schmidt-Rohr, H.W. Spiess, Nature of nonexponential loss of correlation above the glass transition investigated by multi-dimensional NMR, Phys. Rev. Lett. 66 (1991) 3020–3023.
[24] E. Hempel, G. Hempel, A. Hensel, C. Schick, E. Donth, Characteristic length of dynamic glass transition near Tg for a wide assortment of glass forming substances, J. Phys. Chem., B 104 (2000) 2460–2466.
[25] C.-Y. Wang, M.D. Ediger, How long do regions of different dynamics persist in supercooled *o*-terphenyl? J. Phys. Chem., B 103 (1999) 4177–4184.
[26] C.T. Thurau, M.D. Ediger, Influence of spatially heterogeneous dynamics on physical aging of polystyrene, J. Chem. Phys. 116 (2002) 9089–9099.
[27] C.T. Thurau, M.D. Ediger, Change in the temperature dependence of segmental dynamics in deeply supercooled polycarbonate, J. Chem. Phys. 118 (2003) 1996–2004.
[28] M. Le Meste, D. Champion, G. Roudaut, G. Blond, D. Simatos, Glass transition and food technology: a critical appraisal, J. Food Sci. 67 (2002) 2444–2458.
[29] R. Richert, Spectral selectivity in the slow β-relaxation of a molecular glass, Europhys. Lett. 54 (2001) 767–773.
[30] D. Champion, H. Hervet, G. Blond, M. Le Meste, D. Simatos, Translational diffusion in sucrose solutions in the vicinity of the glass transition temperature, J. Phys. Chem., B 101 (1997) 10674–10679.
[31] R. Parker, S.G. Ring, Diffusion in maltose–water mixtures at temperatures close to the glass transition, Carbohydr. Res. 273 (1995) 147–155.
[32] X.-H. Qiu, M.D. Ediger, Length scale of dynamic heterogeneity in supercooled D-sorbitol: comparison to model predictions, J. Phys. Chem., B 107 (2003) 459–464.
[33] L.C. Pravinata, Y. You, R.D. Ludescher, Erythrosin B phosphorescence monitors molecular mobility and dynamic site heterogeneity in amorphous sucrose, Biophys. J. 88 (2005) 3551–3561.
[34] S. Shirke, P. Takhistov, R.D. Ludescher, Molecular mobility in amorphous maltose and maltitol from phosphorescence of erythrosin B, J. Phys. Chem., B 109 (2005) 16119–16126.
[35] K.V. Simon-Lukasik, R.D. Ludescher, Erythrosin B phosphorescence as a probe of oxygen diffusion in amorphous gelatin films, Food Hydrocoll. 18 (2004) 621–630.
[36] K.V. Lukasik, R.D. Ludescher, Effect of plasticizer on dynamic site heterogeneity in cold-cast gelatin films, Food Hydrocoll. 20 (2006) 88–95.
[37] K.V. Lukasik, R.D. Ludescher, Molecular mobility in water and glycerol plasticized cold and hot-cast gelatin films, Food Hydrocoll. 20 (2006) 96–105.
[38] Y. Roos, M. Karel, Plasticizing effect of water on thermal behavior and crystallization of amorphous food models, J. Food Sci. 56 (1991) 38–43.
[39] K. Jouppila, Y.H. Roos, Glass transitions and crystallization in milk powders, J. Dairy Sci. 77 (1994) 2907–2915.
[40] B.C. Hancock, G. Zografi, The relationship between the glass transition temperature and the water content of amorphous pharmaceutical solids, Pharm. Res. 11 (1994) 471–477.
[41] V.L. Hill, D.Q.M. Craig, L.C. Feely, Characterization of spray-dried lactose using modulated differential scanning calorimetry, Int. J. Pharm. 161 (1998) 95–107.
[42] D.Q.M. Craig, M. Barsnes, R.G. Royall, V.L. Kett, An evaluation of the use of modulated DSC as a means of assessing the relaxation behavior of amorphous lactose, Pharm. Res. 17 (2000) 696–700.
[43] M.A. Ottenhof, W. MacNaughtan, I.A. Farhat, FTIR study of state and phase transitions of low moisture sucrose and lactose, Carbohydr. Res. 338 (2003) 2195–2202.
[44] M. Langer, M. Höltje, N.A. Urbanetz, B. Brandt, H.-D. Höltje, B.C. Lippold, Investigations on the predictability of the formation of glassy solid solutions of drugs in sugar alcohols, Int. J. Pharm. 252 (2003) 167–179.
[45] J. McFetridge, T. Rades, M. Lim, Influence of hydrogenated starch hydrolysates on the glass transition and crystallization of sugar alcohols, Food Res. Int. 37 (2004) 409–415.
[46] P.R. Couchman, F.E. Karasz, A classical thermodynamic discussion of the effect of composition on glass transition temperatures, Macromolecules 11 (1978) 117–119.
[47] M. Maroncelli, G.R. Fleming, Picosecond solvation dynamics of coumarin 153: the importance of molecular aspects of salvation, J. Chem. Phys. 86 (1987) 6221–6239.
[48] R. Richert, Triplet state salvation dynamics: basics and applications, J. Chem. Phys. 113 (2000) 8404–8429.

[49] G. Williams, D.C. Watts, Non-symmetrical dielectric relaxation behavior arising from a simple empirical decay function, Trans. Faraday Soc. 66 (1970) 80–85.
[50] C.P. Lindsey, G.D. Patterson, Detailed comparison of the Williams–Watts and Cole–Davidson functions, J. Chem. Phys. 73 (1980) 3348–3357.
[51] R. Duchowicz, M.L. Ferrer, A.U. Acuna, Kinetic spectroscopy of erythrosin phosphorescence and delayed fluorescence in aqueous solution at room temperature, Photochem. Photobiol. 68 (1998) 494–501.
[52] M.P. Lettinga, H. Zuilhof, A.M.J. van Zandvoort, Phosphorescence and fluorescence characterization of fluorescein derivatives in various polymer matrices, Phys. Chem. Chem. Phys. 2 (2000) 3697–3707.
[53] Y. You, R.D. Ludescher, Phosphorescence of erythrosin b as a robust probe of molecular mobility in amorphous solid sucrose, Appl. Spectrosc. (in press).
[54] L.C. Pravinata, M.S. thesis, Rutgers, The State University of New Jersey, New Brunswick, 2003.
[55] A.V. Pastukhov, D.V. Khudyakov, V.R. Vogel, A.I. Kotelnikov, A supercooled glycerol–water mixture: evidence for large scale heterogeneity? Chem. Phys. Lett. 346 (2001) 61–68.
[56] W.R. Ware, S.K. Lee, G.J. Brant, P.P. Chow, Nanosecond time-resolved emission spectroscopy: spectral shifts due to solvent excited solute relaxation, J. Chem. Phys. 54 (1971) 4729–4737.
[57] J.G. Milton, R.M. Purkey, W.C. Galley, The kinetics of solvent reorientation in hydroxylated solvents from the exciting-wavelength dependence of chromophore emission spectra, J. Chem. Phys. 68 (1978) 5396–5404.
[58] R.M. Stratt, M. Maroncelli, Non-reactive dynamics in solution: the emerging molecular view of salvation dynamics and vibrational relaxation, J. Phys. Chem. 100 (1996) 12981–12996.
[59] S. Shirke, R.D. Ludescher, Dynamic site heterogeneity in amorphous maltose and maltitol from spectral heterogeneity in erythrosin B phosphorescence, Carbohydr. Res. 340 (2005) 2661–2669.
[60] R.D. Ludescher, N.K. Shah, C.P. McCaul, K.V. Simon, Beyond Tg: optical luminescence measurements of molecular mobility in amorphous solid foods, Food Hydrocoll. 15 (2001) 331–339.
[61] D. Meißner, J. Einfeldt, Dielectric relaxation analysis of starch oligomers and polymers with respect to their chain length, J. Polym. Sci., Part B, Polym. Phys. 42 (2004) 188–197.
[62] S. Papp, J.M. Vanderkooi, Tryptophan phosphorescence at room temperature as a tool to study protein structure and dynamics, Photochem. Photobiol. 49 (1989) 775–784.
[63] C.J. Fischer, A. Gafni, D.G. Steele, J.A. Schauerte, The triplet state lifetime of indole in aqueous and viscous environments: significance of the interpretation of room temperature phosphorescence in proteins, J. Am. Chem. Soc. 124 (2002) 10359–10366.
[64] G.B. Strambini, M. Gonnelli, The indole nucleus triplet state lifetime and its dependence on solvent microviscosity, Chem. Phys. Lett. 115 (1985) 196–200.
[65] W.J. Jackson, J.R. Caldwell, Antiplasticization: II. Characteristics of antiplasticizers, J. Appl. Polym. Sci. 11 (1967) 211–226.
[66] W.J. Jackson, J.R. Caldwell, Antiplasticization: III. Characteristics and properties of antiplasticizable polymers, J. Appl. Polym. Sci. 11 (1967) 227–244.
[67] D. Lourdin, H. Bizot, P. Colonna, "Antiplasticization" in starch-glycerol films? J. Appl. Polym. Sci. 63 (1997) 1047–1053.
[68] S. Gaudin, D. Lourdin, P.M. Forssell, P. Colonna, Antiplasticization and oxygen permeability of starch–sorbitol films, Carbohydr. Polym. 43 (2000) 33–37.
[69] S. Gaudin, D. Lourdin, D. Le Botlan, J.L. Ilari, P. Colonna, Plasticization and mobility in starch–sorbitol films, J. Cereal Sci. 29 (1999) 273–284.
[70] M.T. Cicerone, A. Tellington, L. Trost, A. Sokolov, Substantially improved stability of biological agents in dried form: the role of glassy dynamics in the preservation of biopharmaceuticals, BioProcess Int. 1 (2003) 36–47.
[71] C.C. Seow, P.B. Cheah, Y.P. Chang, Antiplasticization by water in reduced-moisture food systems, J. Food Sci. 64 (1999) 576–581.
[72] J.S. Vrentas, J.L. Duda, H.-C. Ling, Antiplasticization and volumetric behavior in glassy polymers, Macromolecules 21 (1988) 1470.
[73] D. Lourdin, P. Colonna, S.G. Ring, Volumetric behavior of maltose–water, maltose–glycerol, and starch–sorbitol–water systems mixtures in relation to structural relaxation, Carbohydr. Res. 338 (2003) 2883–2887.
[74] K.L. Ngai, R.W. Rendell, A.F. Yee, D.J. Plazek, Antiplasticization effects on secondary relaxation in plasticized glassy polycarbonates, Macromolecules 24 (1991) 61–67.
[75] D. Lourdin, S.G. Ring, P. Colonna, Study of plasticizer–oligomer and plasticizer–polymer interactions by dielectric analysis: maltose–glycerol and amylose–glycerol–water systems, Carbohydr. Res. 306 (1998) 551–558.
[76] J. Buitink, O. Leprince, Glass formation in plant anhydrobiotes: survival in the dry state, Cryobiology 48 (2004) 215–228.
[77] W. Kauzmann, Dielectric relaxation as a chemical rate process, Rev. Mod. Phys. 14 (1942) 12–44.
[78] R. Zallen, The Physics of Amorphous Solids, Wiley, New York, 1983.
[79] S.R. Elliott, Physics of Amorphous Materials, 2nd ed., Longman Scientific & Technical, Essex, England, 1990.
[80] V. Cody, Conformational analysis of erythrosine B (FD&C Red No. 3) and its comparison with thyroid hormone structure, Endocr. Res. 11 (1985) 211–224.